Reliability Engineering and System Safety 219 (2022) 108217

Contents lists available at ScienceDirect

Reliability Engineering and System Safety

journal homepage: www.elsevier.com/locate/ress

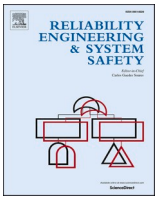

A systematic framework for dynamic nodal vulnerability assessment of water distribution networks based on multilayer networks

Hoese Michel Tornyeviadzi [a,*], Emmanuel Owusu-Ansah [b], Hadi Mohammed [a], Razak Seidu [a]

[a] Department of Ocean Operations and Civil Engineering, Water and Environmental Engineering Group, Norwegian University of Science and Technology, Ålesund, Norway
[b] Department of Mathematics, Kwame Nkrumah University of Science and Technology, Kumasi, Ghana

ARTICLE INFO

Keywords:
Water distribution networks
Node vulnerability
Dynamic vulnerability assessment model
Multilayer networks
Structural reducibility

ABSTRACT

Nodal demands vary throughout the day, as such any vulnerability analysis based on static networks, which considers daily average demands cannot realistically represent the criticality of nodes in the network. This study presents a systematic framework, which couples multilayer networks, structural reducibility and a Demand Adjusted Vulnerability Measure for dynamic nodal vulnerability assessment of water distribution networks (WDNs) under extended period simulation. Within this framework, we present the novel idea of characterizing the dynamics of WDNs with multi-slice networks, which captures the state of the network within a predefined temporal window taking into consideration the directional flow in pipes and the operational status of pumps, valves etc. Using a benchmark WDN, Net 3, as a case study we have demonstrated the importance of demand variations and operational status of various components, no matter how minuscule their operational time, on nodal vulnerability assessment in WDNs. The results indicated that the framework evaluates the criticality of all types of nodes, even intermediary nodes with zero base demand, within any temporal window much more realistically than conventional vulnerability analysis methods based on single (static) networks. Structural reducibility unearthed correlations between the operational status of source nodes and pumps on the general dynamics of the distribution system. The multilayer framework opens a new frontier in vulnerability analysis of WDNs and could serve as a tool for stakeholders in accessing node criticality, impact of various failure scenarios and optimal scheduling of maintenance routines.

1. Introduction

Water distribution networks (WDNs) play a significant role in the socio-economic transformation of many cities by providing a dependable infrastructure for the transportation of potable water for industrial and domestic uses. WDNs are highly interdependent in structure, span different geographical areas and are largely buried underground making them vulnerable to structural failure and attacks [1]. Nodes are essential components of WDNs. They can either serve in the capacity of source nodes that supply water to all other nodes in the WDN, intermediate nodes facilitating the connectivity structure of the network or demand nodes that supply water directly to different entities [2]. The interdependencies between these nodes, make them extremely vulnerable to systemic risks and cascading failures [3]. An interruption or damage to a single node could significantly affect the performance of the distribution network [4] and leave households, schools, hospitals and critical facilities without water.

WDNs are dynamic in nature [5]. The operational status of valves and pumps, variations in nodal demand and pressure dictate the magnitude and direction of flow in the pipelines. In a typical WDN, critical components such as sources, pumps, valves, tanks and auxiliary reservoirs are largely characterised as nodes [6]. Most of these components only become operational when needed. The dynamic and time dependant operational nature of these critical components make the consequences of nodal failure a function of time. For example, failure of the source node and its associated pump in a temporal window where it is not operational will have virtually no impact on the network. Also due to variations in flow directions, the interdependency amongst nodes vary significantly with time. It is important to highlight the fact that the failure impact(s) of a particular node at time t, might not be necessarily the same at time, $t + \delta t$. Specifically, the time of failure of a node dictates the severity of its impact on the WDN.

* Corresponding author.
E-mail address: hoese.m.tornyeviadzi@ntnu.no (H.M. Tornyeviadzi).

https://doi.org/10.1016/j.ress.2021.108217
Received 9 September 2020; Received in revised form 30 June 2021; Accepted 14 November 2021
Available online 22 November 2021

The quantification of node failure impact and the inability of WDNs to cope with failures have been studied using vulnerability assessment methods. Vulnerability assessment methods that examine the vulnerability of individual nodes in WDNs are referred to as local methods [7]. This study belongs to this family of vulnerability assessment methods. These methods can be grouped into 3 categories; (1) topological methods, (2) hydraulic methods and (3) hybrid methods that integrate both topological and hydraulic metrics. Topological vulnerability assessment methods rely solely on the topological characteristics of WDNs to estimate the vulnerability of nodes and the entire distribution system. Meng et al. [8] highlighted key topological attributes such as network centrality, efficiency, modularity, and connectivity responsible for resilient water distribution systems. Yazdani and Jeffrey [4] used meshedness coefficient to quantify the vulnerability of some benchmark WDNs. Some studies have also adopted topological metrics such as clustering coefficient [9], and cospanning edge betweenness [10].

Agathokleous et al. [11] proposed a vulnerability assessment model for WDNs based on betweenness centrality. Other studies have utilised generic centrality measures such as closeness centrality [12,13], edge betweenness centrality [13,14] and entropy of these centrality measures [15,16] to quantify the vulnerability of WDNs. Even though topological metrics provide a quick approximation of vulnerability indexes in the face of limited data [17,18], they do have some limitations. Most topological metrics are based on shortest paths in the distribution system. WDNs have multiple sources and cyclic paths (loops) which introduce significant bottlenecks in shortest path computations. This phenomenon incapacitates topological metrics which do not account for loops and multiple sources in assessing the vulnerability of these types of WDNs [19]. Additionally, water does not necessarily traverse the shortest path, but rather its traversal is based on pressure difference and other parameters [20].

Hydraulic vulnerability assessment measure the vulnerability of WDNs based on the hydraulics of WDNs. Wright et al. [21] proposed a vulnerability metric based on reverse capacity. A new resilience index based on energetic redundancy was proposed by Todini [22]. Other studies [23,24] have presented modifications to Todini's resilience measure. Tanyimboh et al. [25] examined the efficacy of surrogate measures such as statistical entropy, hydraulic reliability, failure tolerance, and resilience index for the hydraulic reliability and redundancy of WDNs. Majority of these hydraulic methods focus exclusively on the hydraulic parameters (pressure, flow, and demand) at the expense of topological attributes. Due to the complex interactions amongst many subsystems and components of WDNs, exclusive hydraulic analysis partially describes the network performance [26] leading to incomplete vulnerability assessment.

In an attempt to resolve this problem, recent studies have resulted to the integration of both topological and hydraulics parameters. Shuang et al. [3] presented a framework for nodal vulnerability analysis based on topological loss and demand deficit. Wang et al. [2] evaluated the vulnerability of nodes based on the amalgamation of two metrics; structural importance quantified by flow betweenness centrality and functional importance quantified by demand deficit. Hybrid approaches based on probabilistic failure rate of segments (a small collection of pipes and nodes) and relative loss in consumption have also been proposed [7,27]. Other methods such as demand centrality [28], and entropy of demand adjusted topological metrics [29] have also been proposed. Maiolo et al. [30] quantified the vulnerability of pipes in WDNs as a linear combination of normalised average flow per pipe and a metric defined on the arcs in the WDN.

It is also important to highlight the fact that majority of the abovementioned studies have abstracted WDNs as static networks which completely ignore their dynamic nature which accounts for variations in demand and operational status of various assets of the WDN. Vulnerability measures that consider just one snapshot analysis of the network (peak demands or daily average) cannot quantify the overall system vulnerability realistically [31]. In order to holistically evaluate nodal vulnerability, topological parameters, hydraulic parameters, and the dynamic components of WDNs must be considered simultaneously in the development of vulnerability assessment tools. To the best of our knowledge the dynamic facets of the distribution system has not been explicitly considered by prior studies in local vulnerability assessment of WDN components. In addition, most topological metrics utilized in vulnerability assessment do not account for WDNs with cyclic paths (loops) & multiple sources. Examining nodal vulnerability in WDNs from a dynamic perspective has some advantages over the static methods. Nodal demand variations and the criticality of each component of the WDN, no matter how minuscule its operational time, is considered in the vulnerability assessment. Vulnerability estimates of nodes accounting for time will present an opportunity for managers of WDNs to optimally schedule maintenance routines within the day to avoid prolonged service downtime/disruptions and minimise customer dissatisfaction [24].

This study proposes a systematic framework for dynamic nodal vulnerability assessment of WDNs. The framework is implemented in three phases. In phase one, each dynamic facet of the distribution system is captured in discrete time via multi-layer networks [32] where each layer of the network represents the state of the WDN within a temporal window (e.g. an hour). Network science has shown that characterising complex dynamic systems with multilayer networks is fundamental in the comprehension of these systems [33]. To the best of our knowledge, WDNs are seldom characterised by multilayer networks. However, multilayer networks have been utilised extensively to study the spreading of information on social networks [34], the robustness and reliability of transportation networks [35,36], percolation in power grids [37,38] and disease transmission in biological networks [39,40]. These multilayer networks are known to retain multi-dimensional information [35], reveal hidden structural properties [41,42] and sometimes new physical phenomena not previously considered [43,44].

In phase two, structural reducibility of multilayer networks [45] is adopted to aggregate similar layers with minimal information loss, eliminate redundancy and maximize the distinguishability between aggregated networks [45,46]. Structural reducibility is crucial due to the fact that all path-based measures in multilayer networks scale exponentially with the number of layers [47]. Failure to structurally reduce multilayer networks could potentially render medium-sized networks computationally infeasible [45] and hinder their application to real-world water distribution systems. The aggregation of similar layers is also known to unearth hidden and implicit correlations, patterns, and dynamics in the network.

Phase three focuses on nodal vulnerability estimation of each node in each layer of the aggregated network using a novel hybrid Demand Adjusted Vulnerability Measure (DAVM). DAVM, which is based on topological connectivity loss and demand deficit due to nodal failure, has the propensity to handle WDNs with cyclic paths (loops), multiple sources and simultaneous failure of multiple nodes. The utilisation of DAVM ensures that these inherent topological characteristics of WDNs are explored in the vulnerability analysis. These three phases would then be synthesised to realise dynamical vulnerability assessment in WDNs.

The main assumptions considered in this study are; (a) all nodes have equal probability of failure at any time t, (b) failure events occur in discrete time and are confined to a specific temporal window and (c) node failure does not cause flow reduction or redistribution in paths that do not contain this particular node. These assumptions are considered because the impact of failure events can only be ascertained in discrete time and in many cases proper technical or managerial measures can be taken in a timely manner to avoid the amplification of failure effects in the distribution network [2]. The overarching aim of this paper is to assess the nodal vulnerability in WDNs from a dynamical point of view with much emphasis on time and its implications on the diverse dynamic facets of the distribution system.

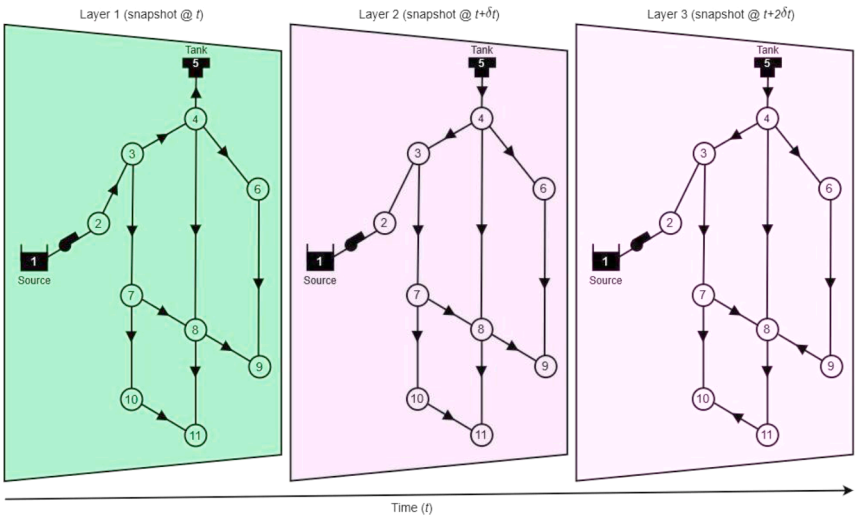

Fig. 1. Net 1 in EPANET represented as a multi-slice network.

2. Methods and materials

2.1. Multi-layer networks

Multilayer networks have been used to study the dynamics of complex systems interacting at comparable time scales [45]. The temporal structure of edge/link activations affect the dynamics of information flow in the network. As such, snapshots of the same network through time exhibit different interaction properties. These snapshots are referred to as the layers of the multilayer network. A multilayer network is defined mathematically as [48]

$$M = \left(Y, \overrightarrow{G}, G\right) \tag{1}$$

Where $Y = \{\alpha | \alpha \in \{1, 2, 3, \ldots, m\}\}$ represents the set of layers in the multilayer network. $\overrightarrow{G}$ is the ordered list of networks characterizing the interactions within each layer. Thus, $\overrightarrow{G} = (G_1, G_2, \ldots, G_m)$ and $G_\alpha = (V_\alpha, E_\alpha)$ represents the network in each layer, Y_α. The set of vertices and edges in Y_α are represented by V_α and E_α, respectively. G is a list of $m \times m$ bipartite networks characterizing the interactions across different layers and has the elements $G_{\alpha,\beta} = (V_\alpha, V_\beta, E_{\alpha,\beta})$. $E_{\alpha,\beta}$ represents an edge connecting vertices in layer α to vertices in layer β. Multilayer networks are generally classified as either multiplex networks, network of networks or multi-slice networks [49]. The most suitable form of multilayer networks for WDNs is the multi-slice networks.

2.1.1. Multi-slice networks

A multi-slice network is a special type of multilayer networks in which there is one-to-one mapping of vertices in different layers. Thus, the vertices replicate themselves across different layers and each layer is a snapshot of the temporal network. Each layer has the same set of vertices but the interactions (edge activations) differ in different layers. For example, there could be an edge/interaction between vertices a and b at time, t but this edge/interaction becomes non-existent at time, $t + \delta t$. In the context of WDNs under extended period simulation, these edge/link activations represent the directional flow of water in the pipes and operational status of the components in the network. Fig. 1 represents snapshots of a dummy WDN within different temporal windows. The interactions exhibited determine the vulnerability of the nodes in the WDN.

Each layer corresponds to the state of the network within a temporal window δt. The interactions between nodes are the unique flow directions in each temporal window. The nodes replicate themselves across all snapshots, but the directional flow and operational status of the source, pump and tank differ.

In the absence of connections/links between different layers, a multi-slice network is defined mathematically as

$$M = \left(Y, \overrightarrow{G}\right) \tag{2}$$

Where $\overrightarrow{G} = (G_1, G_2, \ldots, G_m)$ and $G_\alpha = (V_\alpha, E_\alpha)$ represents the interactions occurring in a time window δt. The interactions character-

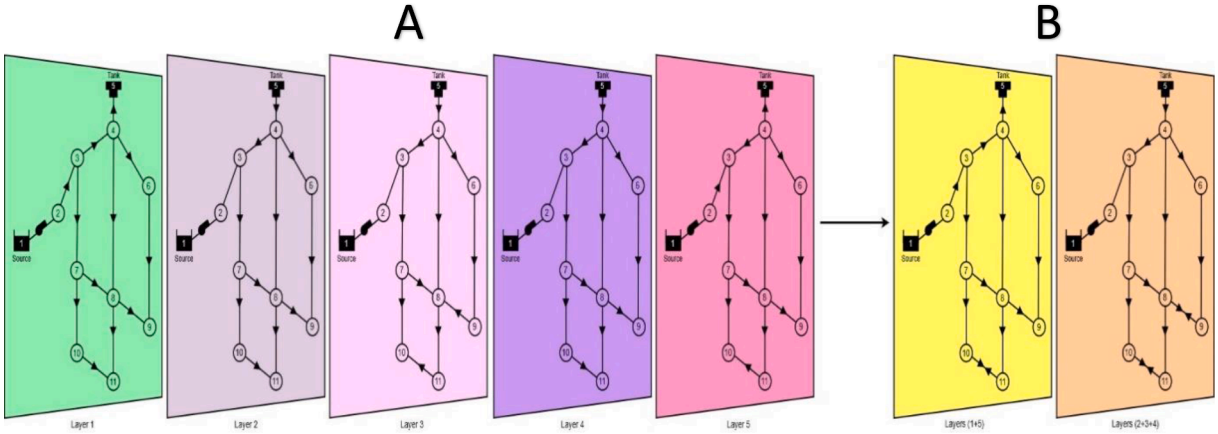

Fig. 2. **A:** Original multilayer network, **B:** Reduced multilayer network.

izing each time window describes each layer in the network. Each layer is fully characterized by an $N \times N$ adjacency matrix, $A^{[\alpha]}$ with $\alpha = 1,2,\ldots, m$. We restrict the interactions in each layer to be directed to suit WDNs. The adjacency matrix of any arbitrary layer α is defined as

$$A_{ij}^{[\alpha]} = \begin{cases} 1, \ if \ node \ i \ connects \ to \ node \ j \ in \ the \ time \ window \ [t+(\alpha-1)\delta t, t+\alpha\delta t) \\ 0, \ otherwise \end{cases} \tag{3}$$

2.2. Structural reducibility of multi-layer networks

Even though multilayer networks present a new frontier for analysing complex dynamic systems, they are sometimes plagued with information redundancy. There is the possibility of having identical interactions on a dynamic system within two separate time windows. The layers representing these temporal windows carry the same information. It is therefore important to find a representation of the layers that minimize redundancy. Given a multilayer network of size m characterising a dynamic system, structural reducibility is concerned with finding an optimal configuration consisting of minimal number of layers, n, that accurately describes the dynamics of the system with virtually no information loss. The number of layers in the reduced multilayer network is expected to be less or equal to the number of layers in the original multilayer network ($n \leq m$).

In WDNs under extended period simulation, the characteristics/states of the distribution system could replicate itself within different time windows. The nodal demand and operational status of some the components of the network could be identical in successive time windows or different time windows. For example, Fig. 2 presents a hypothetical multilayer representation of Net 1 in EPANET with redundant layers. Layers 1 and 5 are similar with the only exception being the directional flow between nodes 10 and 11. A similar pattern can be seen in layers 2,3 and 4. The original multilayer network of size five has been reduced to two layers that optimally describe the evolution of the network.

The procedure to structurally reduce multilayer networks is outlined as follows [45];

Step 1: Compute the Jensen-Shannon divergence metric

This divergence metric quantifies the dissimilarity between all pairs of layers in the multilayer network and has a range of (0–1). Identical layers have a Jensen-Shannon divergence metric of zero. The pair of layers having zero or infinitesimally small divergence metric value is a prime candidate for aggregation. Given two layers, α and β, of a multilayer network associated with density matrices $\rho_\alpha$and ρ_β respectively, the Jensen-Shannon divergence metric, D_{JS}, is a linear combination of the Kullback-Liebler divergence metric, D_{KL}, between layer α and layer β, and that of layer β and layer α.

$$D_{JS}(\rho_\alpha \| \rho_\beta) = \frac{1}{2} D_{KL}(\rho_\alpha \| \rho_\beta) + \frac{1}{2} D_{KL}(\rho_\beta \| \rho_\alpha) \tag{4}$$

This linear combination stems from the fact that the Kullback-Liebler divergence metric is an asymmetric measure of how different layer α is from layer β. D_{KL} is mathematically expressed as

$$D_{KL}(\rho_\alpha \| \rho_\beta) = \mathrm{Tr}\left[\rho_\alpha \left(\log_2(\rho_\alpha) - \log_2(\rho_\beta)\right)\right] \tag{5}$$

The density matrix associated with a specific layer, say ρ_α, is the degree normalised Laplacian which the takes the form

$$\rho_\alpha = \frac{D^{[\alpha]} - A^{[\alpha]}}{2K^{[\alpha]}} \tag{6}$$

Where $D^{[\alpha]}$ is a diagonal matrix of node degrees of layer α, $A^{[\alpha]}$ is the adjacency matrix of layer α and $K^{[\alpha]}$ is the number of links in layer α.

Step 2: Hierarchical clustering of identical layers

Hierarchical clustering is adopted to group similar layers based on the Jenson-Shannon divergence metric. At each step of the greedy hierarchical clustering algorithm, any two clusters of layers separated by the smallest value of D_{JS}, are aggregated. After which the distances between the newly formed cluster and the remaining ones are updated according to the Ward's linkage function [50]. The procedure is repeated until all similar layers in the network are aggregated. The distinguishability of the reduced multilayer network is quantified by its relative entropy when compared with the original multilayer network. The relative entropy, $q(\cdot)$, is defined as

$$q(C) = 1 - \frac{-\frac{1}{n}\sum_i^n \mathrm{Tr}\left[\rho_{C^{[i]}} \log_2 \rho_{C^{[i]}}\right]}{-\mathrm{Tr}[\rho_A \log_2 \rho_A]} \tag{7}$$

Where $C = \{C^{[1]}, C^{[2]}, \cdots, C^{[n]}\}$ represents the reduced multilayer network, and $A = \{A^{[1]} + A^{[2]} + \cdots + A^{[n]}\}$ denotes the aggregation of all layers of the original multilayer network. The larger the magnitude of (C), the more distinguishable the reduced multilayer network C from A. If all the layers of C are identical to that of A, then $q(C) = 0$, implying that $C = A$. Conversely, $q(C) > 0$ indicates that the reduced multilayer network with n layers is distinguishable from the aggregated multilayer network. The hierarchical clustering algorithm therefore seeks to maximize the relative entropy of the reduced multilayer network.

See Domenico et al. [45] for further details on the algorithm utilized for structural reducibility of multilayer networks. A python implementation of the code is available at https://github.com/KatolaZ/multired.

2.2.1. Layer aggregation

In the context of this study, layer aggregation refers to the combination of similar layers of a multilayer network into a single layer. An aggregated layer $\widetilde{G} = (V, \widetilde{E})$ is formed by replica nodes of a multi-slice network and has a set of links $\widetilde{E}$ across the aggregated layers. $\widetilde{G}$ is characterized by an adjacency matrix $\widetilde{A}$ that has entries $\widetilde{A}_{i,j} = 1$ if and only if the edge (i,j) exists in at least one layer. i.e.

$$\widetilde{A}_{i,j} = \begin{cases} 1, \ if \ \sum_{\alpha=1}^{m} A_{i,j}^{[\alpha]} > 0 \\ 0, \ otherwise \end{cases} \tag{8}$$

The aggregated layer represents temporal windows in which the general dynamics of the WDN is identical/similar. There could be instances where the flow direction in some pipes are different. Both directions are represented by the merged/aggregated layer but only the dominant flow direction is utilized in the vulnerability analysis. We acknowledge the fact that neglecting the less dominant flow direction could result in some information loss. However, it must be noted that the dominant flow direction is the flow direction that persists in the aggregated temporal windows. We believe the dominant flow direction is a good candidate to represent the flow direction of the aggregated temporal windows.

2.3. Demand Adjusted Vulnerability Measure

Demand adjusted Vulnerability Measure (DAVM) is a hybrid nodal vulnerability index based on connectivity loss of the topological structure and demand deficit created in the WDN as a result of node failure. Node failure is defined as the inability of a node to deliver service (required demand) which is most often triggered by pipe burst, pump, or valve damage. Node failure is simulated by removing the affected node from the rest of the network and its connected pipes (i.e., the outflow pipes and the inflow pipes) closed. This approach has been used by previous studies [2,3] to operatively simulate node failure in WDNs. From a topological point of view, failure of a node does not sequentially impact all nodes directly connected to this node but rather all paths that contain this node become invalid. Connectivity Loss (CL) in the context of DAVM is defined as the fraction of the network invalidated due to failure of a node. CL of node k is mathematically defined on a directed

Algorithm 1
Number of Impacted Nodes.

1. Given $G(v,e)$
2. $nn = |v|$
3. **for** $i = 1 : nn$
4. $A \leftarrow$ neighbors(G, i, ∞) //All neighbours of vertex i
5. A $\leftarrow$ [A i] // Concatenate vertex to its neighbors
6. $mm = |A|$, $C = []$
7. **for** $j = 2 : mm$
8. path{j} $\leftarrow$ kShortestPath(G,*source*,$A(j)$,*MaxPaths*) // All shortest paths in A
9. $q = |path|$
10. **for** $k = 1 : q$
11. $B \leftarrow$ find(path{k}==i) // Index B if node i is in path{k}
12. **if** $B = []$
13. $C \leftarrow [C\ A(j)]$ // Concatenate non impacted nodes
14. break
15. **end**
16. **end**
17. **end**
18. **if** $C = []$
19. $D \leftarrow A$ // All neighbors are impacted
20. **else**
21. $D \leftarrow$ setdiff(A, C) // Remove non impacted nodes from neighbors of vertex i
22. **end**
23. $E = |D|$ // Number of impacted nodes
24. ***End***

graph $G(V,\ E)$ as:

$$CL(k) = \frac{n_L}{N_T} \forall\ k \in V \tag{9}$$

Where, n_L is the number of nodes impacted due to failure of node k and $N_T = |V|$ is the total number of nodes in G. Using the concept of reachability in graph theory, all nodes connected to node k can be enumerated. The reachability of node k is defined as the set of reachable nodes from node k on a directed graph $G = (V,E)$.

$$N(k) = \{i \in V :\ \delta_{ki} < \infty\} \tag{10}$$

Where $N(k)$ represent the set of all nodes reachable from node k in G and δ_{ki} represents the distance between node k and node i in G. To find the number of impacted nodes, n_L, due to failure of node k, we iterate through $N(k)$ to see if there is/are path(s) from the source(s) to these nodes that do not traverse node k. If there is/are path(s) from the source (s) to node i in $N(k)$ that do not traverse node k, then node i is not impacted by the failure of node k. In order to improve reliability and limit the impact of node failures, WDNs are designed to have cycles/loops which introduces significant bottlenecks in path computations. A modified Dijkstra Algorithm [51] with the ability to handle cyclic paths (loops) is utilised in the computation of water paths in the network. Algorithm 1 outlines the pseudocode for computing the number of affected/impacted nodes due to failure of a single node k. For distribution networks with multiple sources, Line 10 of Algorithm 1 can be modified to compute the paths from these individual sources.

The computation of the demand deficit due to nodal failure is based on the computation of number of affected nodes in Algorithm 1. The demand deficit at node k, $DD(k)$, is defined as the demand not satisfied due to the failure of n_L number of nodes (affected nodes) initiated by the failure of node k. This demand deficit is computed via EPANET [52]. Mathematically, $DD(k)$ can be expressed as the sum of affected nodal demands at time t. Thus,

$$DD(k) = \sum_{i=1}^{n_L} D_{aff}(i) \tag{11}$$

where D_{aff} is the demand on the affected nodes. Let DM be an array of nodal demands at time t, then $D_{aff} = DM$(Index of affected nodes).

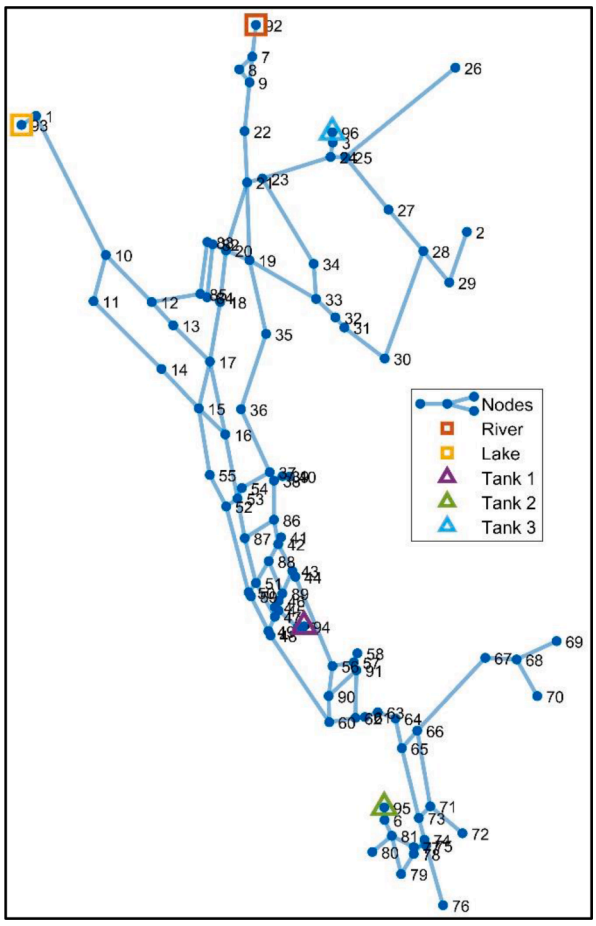

Fig. 3. Net 3.

Typically, WDNs have 3 types of nodes namely; source nodes, intermediary nodes, and demand nodes. Water flows from source nodes to demand nodes through intermediary nodes. These intermediary nodes do not have base demand and only facilitate the connectivity structure of the distribution network. This highlights the need to sum the demand on the paths affected by the failure of node k rather than demand at node k as suggested by other researchers.

Finally, the Demand Adjusted Vulnerability Measure which is a hybrid vulnerability measure that weighs the connectivity loss of node k, $CL(k)$, with its demand deficit, $DD(k)$, is given as

$$DAVM(k) = CL(k) * DD(k \tag{12}$$

Coupling connectivity loss with cumulative demand deficit ensures that the vulnerability of nodes that result in the same connectivity loss are differentiated based on cumulative demand deficit created in the WDN. The failure of any two arbitrary nodes in a WDN could result in the same connectivity loss but their respective cumulative demand deficit might not be the same. The node failures that result in higher cumulative demand deficit must be given much prominence over the others. As such, DAVM weights connectivity loss with demand deficit to make this distinction. Additionally, DAVM ensures that singular sink node failures that result in moderate demand deficit are not over emphasised in comparison to node failures that result in huge connectivity loss with similar cumulative demand deficit.

The Demand Adjusted Vulnerability Measure can be summarised in four steps; (1) Compute Connectivity Loss of node k denoted $CL(k)$, (2) Compute the Demand Deficit of node k denoted $DD(k)$, (3) find the product of $CL(k)$ and $DD(k)$, and (4) rank the Demand Adjusted vulnerability Indexes.

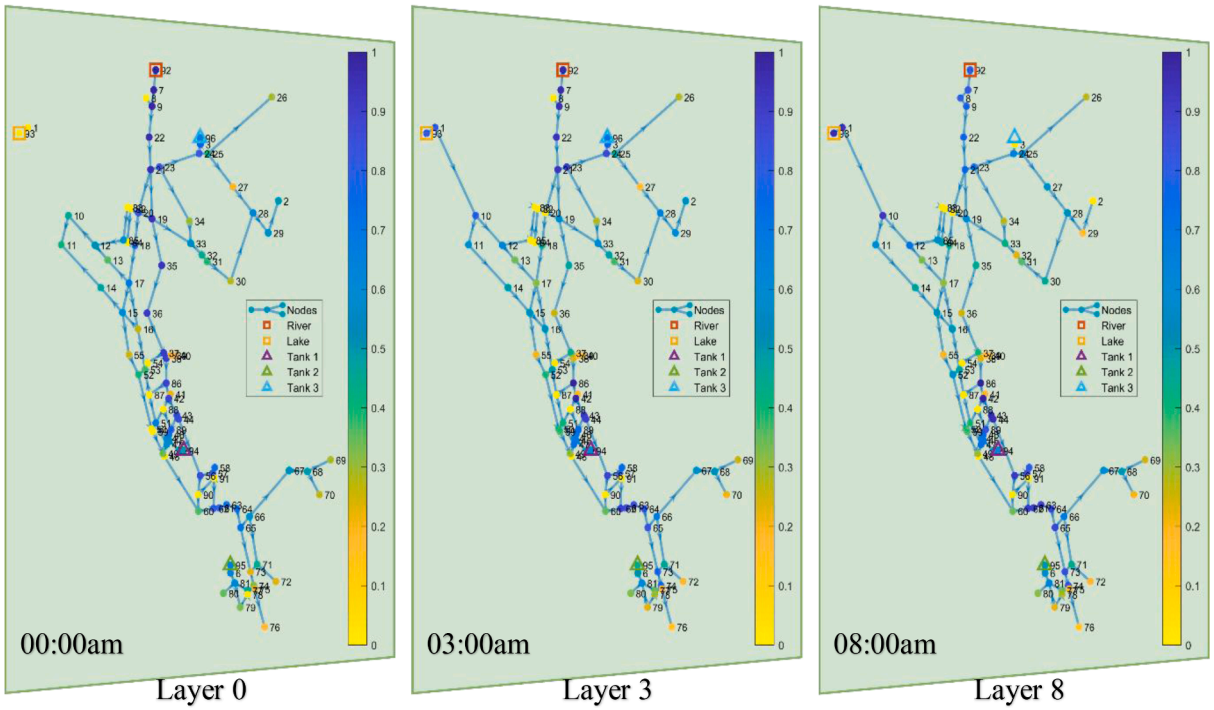

Fig. 4. Layers 0, 3 and 8 of the multilayer representation of Net 3.

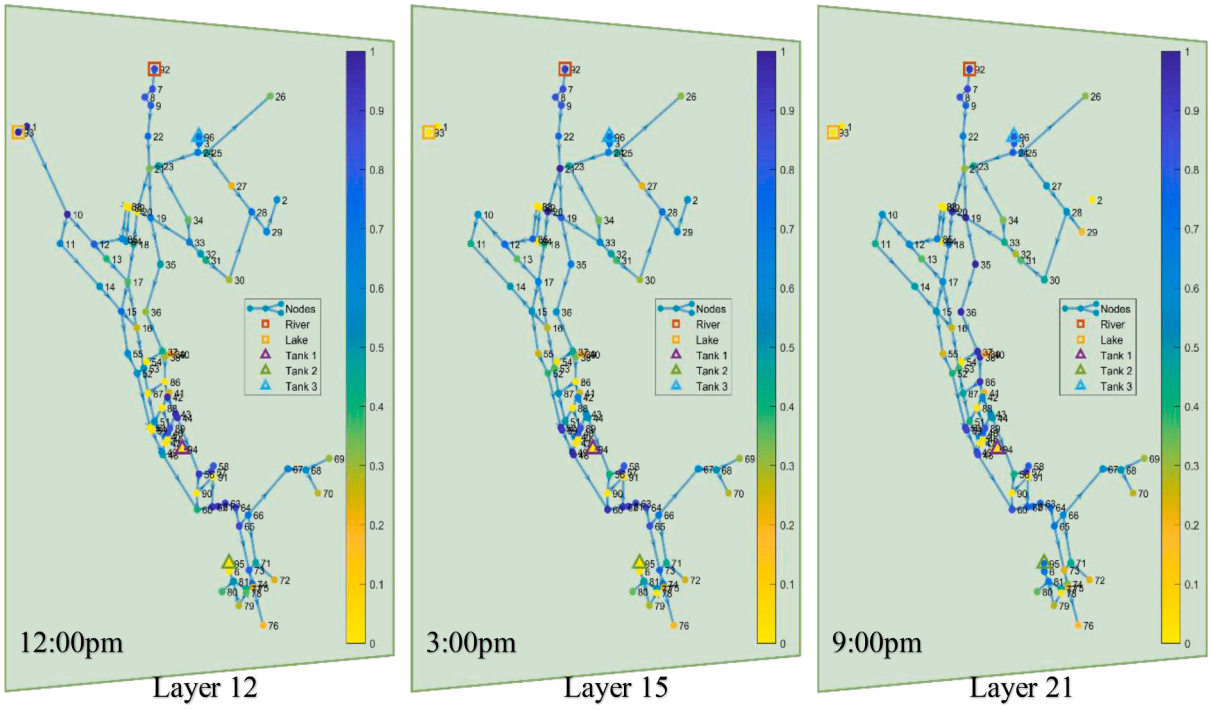

Fig. 5. Layers 12, 15 and 21 of the multilayer representation of Net 3.

3. Case study

To demonstrate the applicability and efficacy of the proposed framework, a standard benchmark WDN extensively used in literature, North Marin Water District Network, California-USA [53] popularly called Net 3, is chosen as a case study. Net 3 has 3 tanks, 2 pumps, two sources and 97 nodes as shown in Fig. 3. The choice of Net 3 is influenced by its characteristics. It has multiple sources which add significant complexities in nodal vulnerability estimation [28]. Net 3 affords us the opportunity to demonstrate some of the exceptional capabilities of DAVM and achieve tractability.

Using the EPANET-MATLAB-Toolkit [54] an extended period simulation is carried out for a period of 24 hours. This specific period is chosen in order to ascertain holistically the vulnerability of each dynamic component of the WDN. It is expected that within this period each component of the network might have been operational at least once. A

Table 1
Kendall's rank correlation coefficient of Layers 0 to 23 of Net 3.

	L_0	L_1	L_2	L_3	L_4	L_5	L_6	L_7	L_8	L_9	L_{10}	L_{11}	L_{12}	L_{13}	L_{14}	L_{15}	L_{16}	L_{17}	L_{18}	L_{19}	L_{20}	L_{21}	L_{22}	L_{23}
$\mathbf{L_0}$	1	0.654	0.593	0.593	0.591	0.492	0.549	0.475	0.409	0.387	0.387	0.378	0.378	0.401	0.432	0.419	0.343	0.344	0.350	0.403	0.493	0.531	0.672	0.790
$\mathbf{L_1}$		1	0.909	0.910	0.869	0.714	0.772	0.681	0.669	0.574	0.572	0.561	0.561	0.579	0.627	0.375	0.298	0.299	0.305	0.315	0.315	0.308	0.426	0.552
$\mathbf{L_2}$			1	0.998	0.943	0.743	0.802	0.700	0.714	0.583	0.581	0.579	0.578	0.600	0.654	0.356	0.292	0.293	0.304	0.300	0.262	0.251	0.363	0.499
$\mathbf{L_3}$				1	0.944	0.745	0.803	0.699	0.715	0.583	0.580	0.577	0.576	0.598	0.653	0.355	0.292	0.293	0.304	0.300	0.263	0.252	0.364	0.501
$\mathbf{L_4}$					1	0.769	0.828	0.717	0.743	0.595	0.593	0.593	0.593	0.613	0.668	0.339	0.275	0.275	0.286	0.280	0.262	0.252	0.366	0.472
$\mathbf{L_5}$						1	0.934	0.797	0.755	0.772	0.772	0.773	0.774	0.799	0.870	0.324	0.294	0.294	0.298	0.291	0.244	0.233	0.357	0.363
$\mathbf{L_6}$							1	0.856	0.778	0.746	0.741	0.741	0.740	0.766	0.833	0.346	0.288	0.287	0.291	0.285	0.240	0.228	0.375	0.421
$\mathbf{L_7}$								1	0.809	0.850	0.849	0.689	0.688	0.713	0.776	0.321	0.377	0.377	0.380	0.371	0.313	0.297	0.347	0.383
$\mathbf{L_8}$									1	0.714	0.714	0.569	0.568	0.590	0.660	0.270	0.321	0.321	0.331	0.322	0.277	0.268	0.278	0.305
$\mathbf{L_9}$										1	0.981	0.814	0.812	0.819	0.844	0.384	0.492	0.491	0.493	0.437	0.330	0.291	0.281	0.303
$\mathbf{L_{10}}$											1	0.812	0.813	0.833	0.853	0.383	0.491	0.490	0.492	0.436	0.341	0.301	0.285	0.314
$\mathbf{L_{11}}$												1	0.998	0.968	0.870	0.525	0.494	0.493	0.485	0.447	0.332	0.294	0.299	0.412
$\mathbf{L_{12}}$													1	0.966	0.869	0.524	0.492	0.491	0.483	0.445	0.330	0.292	0.298	0.411
$\mathbf{L_{13}}$														1	0.900	0.501	0.471	0.470	0.475	0.423	0.342	0.301	0.316	0.424
$\mathbf{L_{14}}$															1	0.420	0.382	0.382	0.385	0.336	0.275	0.234	0.337	0.364
$\mathbf{L_{15}}$																1	0.849	0.849	0.835	0.797	0.674	0.622	0.435	0.506
$\mathbf{L_{16}}$																	1	0.999	0.981	0.931	0.781	0.727	0.340	0.424
$\mathbf{L_{17}}$																		1	0.982	0.933	0.781	0.728	0.342	0.426
$\mathbf{L_{18}}$																			1	0.921	0.789	0.735	0.349	0.433
$\mathbf{L_{19}}$																				1	0.841	0.791	0.408	0.489
$\mathbf{L_{20}}$																					1	0.938	0.524	0.595
$\mathbf{L_{21}}$																						1	0.578	0.632
$\mathbf{L_{22}}$																							1	0.703
$\mathbf{L_{23}}$																								1

steady state simulation is unable to capture the diverse dynamic aspects of the WDN. The concept of multi-slice networks is then adopted to characterise Net 3 as a multilayer network with 24 layers. Each layer represents a 1-hour temporal window. Using flow in the pipes, each layer of the multi-slice network is abstracted as a directed graph. Abstracting each layer as a directed graph implies that all the hydraulic attributes of the WDN are implicitly considered. To ensure thorough analysis, the failure impact of each node in each layer of the WDN in terms of connectivity loss and demand deficit is evaluated.

4. Results and discussions

4.1. Multilayer vulnerability assessment

The vulnerability of each node in each layer of the multilayer network is evaluated using DAVM (see supplementary materials for detailed DAVM tables and vulnerability colour map for each of the 24 layers). In this subsection, we present some of the layers (Figs. 4 and 5) and discuss them thoroughly. These discussions can be generalised to the other layers. The colour scale represents the criticality index of the nodes. One representing the most vulnerable and zero representing the least vulnerable.

From layer 0 in Fig. 4, the second source of Net 3, the lake and the pump associated with it are not operational since there is no flow in the pipes linking them. Using flows in the pipes we can ascertain the operational status of various components in the WDN. If the flow in a particular pipe is zero, it implies the component attached to this pipe is non-operational. It is obvious that the failure of second source denoted as Node 93 and its associated pump will have no effect on the entire network in this particular temporal window. These components are the least vulnerable in layer 0 as indicated by the colour bar. The main source, Node 92 is the most vulnerable node in Layer 0. From a functional viewpoint, Node 92 supplies the entire fleet of nodes in the network within this temporal window. Its failure will have catastrophic consequences since the entire network will be disrupted. The 2nd and 3rd most vulnerable nodes are Nodes 7 and 9, respectively. These intermediate nodes have zero base demand but facilitate the connectivity structure of the network. We have been able to capture accurately the vulnerability of these nodes due to the fact that DAVM sums all the nodal demands on the affected nodes in the reachability graph of these nodes. DAVM captures the vulnerability associated with any kind of node in the network, be it source nodes, intermediate nodes, or demand nodes. Given any two sink nodes, DAVM can distinguish between their vulnerabilities based on their nodal demands. A sink node with a higher nodal demand is deemed more vulnerable since nodal demand can be used as an estimate of the number of entities impacted by the failure of a particular node. This explains why the various sink nodes in the network have different colour codes signifying different vulnerability indexes.

In layer 3, both sources of the network are operational. However, Node 92 is more vulnerable than Node 93 due to the fact that the volume of water supplied by Node 92 is significantly larger. The pumps associated with each of these sources are also operational. DAVM is able to capture the criticality of these two sources operating simultaneously. According to the colour map, Node 86 has a high vulnerability index. This is due the fact that the number of nodes in the reachability graph of Node 86 is fairly large and both sources supply water through Node 86 to majority of the nodes downstream of Node 86. In this instance, Node 86 is acting as an intermediary for all the nodes in its reachability graph. Without Node 86 it will be impossible to reach any of these nodes. In layer 8, Node 93 is highly vulnerable. This stems from the fact that the link between Nodes 7 and 9 has zero flow indicating the pump associated with Node 92 is not operational. Therefore, the entire fleet of nodes in the network is largely supplied by Node 93. Node 92 is using the bypass pipe to supply the network. Similarly, in layer 12, Node 93 is the most vulnerable. Interestingly, Node 96 (Tank 3) is also supplying water. Comparing layers 8 and 12 it is obvious that the vulnerability index of

Table 2
90th to 100th percentile vulnerability ranking of nodes in each layer of Net 3. (Nd = Node).

Rank	L_0	L_1	L_2	L_3	L_4	L_5	L_6	L_7	L_8	L_9	L_{10}	L_{11}	L_{12}	L_{13}	L_{14}	L_{15}	L_{16}	L_{17}	L_{18}	L_{19}	L_{20}	L_{21}	L_{22}	L_{23}
1	Nd	Nd	Nd	Nd	Nd	Nd	Nd	Nd	Nd	Nd	Nd	Nd	Nd	Nd	Nd	Nd	Nd	Nd	Nd	Nd	Nd	Nd	Nd	Nd
	92	86	86	86	86	86	86	93	86	93	93	93	93	93	93	21	49	49	50	49	20	19	21	92
2	Nd 7	Nd	Nd	Nd	Nd	Nd	Nd	Nd 1	Nd	Nd 1	Nd 1	Nd 1	Nd 1	Nd 1	Nd 1	Nd	Nd	Nd	Nd	Nd	Nd	Nd	Nd	Nd 7
		42	42	42	42	42	42		42							49	20	20	59	20	92	35	19	
3	Nd 9	Nd	Nd	Nd	Nd	Nd	Nd	Nd	Nd	Nd	Nd	Nd	Nd	Nd	Nd	Nd	Nd	Nd	Nd	Nd	Nd	Nd	Nd	Nd 9
		92	92	92	92	43	43	10	43	10	10	10	10	10	10	20	48	48	49	48	57	36	35	
4	Nd	Nd 7	Nd 7	Nd 7	Nd 7	Nd	Nd	Nd	Nd	Nd	Nd	Nd	Nd	Nd	Nd	Nd	Nd	Nd	Nd	Nd	Nd 7	Nd	Nd	Nd
	22					44	44	86	93	42	42	42	42	42	42	48	60	60	48	60		37	36	22
5	Nd	Nd 9	Nd 9	Nd 9	Nd 9	Nd	Nd	Nd	Nd	Nd	Nd	Nd	Nd	Nd	Nd	Nd	Nd	Nd	Nd	Nd	Nd	Nd	Nd	Nd
	21					93	56	42	44	43	43	43	43	43	43	60	50	50	20	50	50	38	37	21
6	Nd	Nd	Nd	Nd	Nd	Nd 1	Nd	Nd	Nd 1	Nd	Nd	Nd	Nd	Nd	Nd	Nd	Nd	Nd	Nd	Nd	Nd	Nd	Nd	Nd
	19	22	22	22	22		93	43		44	44	44	44	44	44	50	59	59	60	92	59	86	38	19
7	Nd	Nd	Nd	Nd	Nd	Nd	Nd 1	Nd	Nd	Nd	Nd	Nd	Nd	Nd	Nd	Nd	Nd	Nd	Nd	Nd	Nd	Nd	Nd	Nd
	35	43	21	21	21	56		44	10	62	62	62	62	62	62	62	62	62	92	57	49	20	86	35
8	Nd	Nd	Nd	Nd	Nd	Nd	Nd	Nd	Nd	Nd	Nd	Nd	Nd	Nd	Nd	Nd	Nd	Nd	Nd	Nd	Nd	Nd	Nd	Nd
	36	21	43	43	23	10	10	92	56	56	56	56	56	56	56	59	92	92	62	59	19	92	42	36
9	Nd	Nd	Nd	Nd	Nd	Nd	Nd	Nd 7	Nd	Nd	Nd	Nd	Nd	Nd	Nd	Nd	Nd	Nd	Nd	Nd	Nd 8	Nd	Nd	Nd
	37	44	23	23	43	62	62		62	61	61	61	61	61	61	92	57	57	57	62		57	92	37
10	Nd	Nd	Nd	Nd	Nd	Nd	Nd	Nd	Nd	Nd	Nd	Nd	Nd	Nd	Nd	Nd	Nd	Nd	Nd	Nd 7	Nd	Nd	Nd	Nd
	38	23	44	44	24	61	61	62	61	63	63	63	63	63	63	57	61	61	61		48	50	57	38

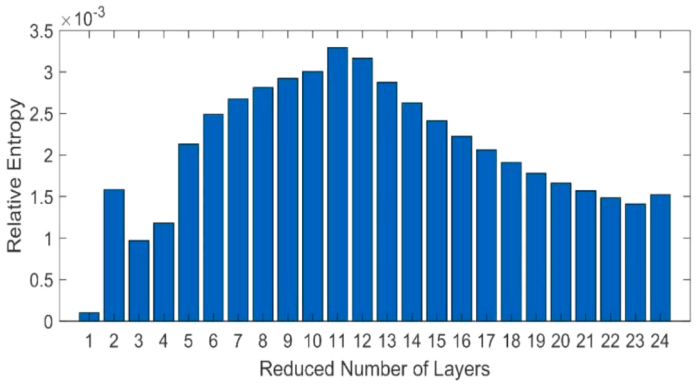

Fig. 6. Relative Entropy of Reduced MultiLayer networks.

Node 96 has appreciated in layer 12.

Node 93 and its associated pump are not operational in layer 15 as such they are the least vulnerability nodes. As partly explained in the discussion of layer 3, Node 21 is deemed the most vulnerable node by DAVM in layer 15. This is inherently due to how DAVM is formulated. DAVM assumes that when a node fails, its failure only impacts the water paths that contain this particular node. The failure of Node 92 will not have significant impact on the network since Node 96 is also supplying. Same can be said of the failure of Node 96 since Node 92 will also be supplying. However, failure of Node 21 will invalidate more than 80% of the entire network due to how gigantic the reachability graph of Node 21 is. Additionally, Nodes 92 and 93 which are the only nodes supplying water in layer 15 deliver water to about 80% of the nodes in the network through Node 21. Unless Nodes 92 and 93 fail simultaneously, Node 21 is considered the most vulnerable node. Even though DAVM is capable of evaluating vulnerability indexes of WDNs with multiple nodal failure, the associated computational cost does not warrant its consideration in this study. Similar to layer 15, Node 19 is deemed the most vulnerable node in layer 21. This is mainly due to changes in nodal demand and directional flows in the pipes. The vulnerability index of Node 95 (Tank 2) has appreciated significantly when compared with previous layers. This is because in layer 21, Node 95 is supplying water.

Table 1 presents the Kendall's rank correlation coefficient, a non-parametric measure of ordinal association between the criticality ranking of nodes in different layers of the network. A perfect correlation coefficient of 1 implies that the vulnerability ranking of nodes in any two layers are identical. Almost perfect correlation can be noted between layers 3 and 4, layers 11 and 12, and layers 16 and 17. This is an indication that the vulnerability ranking of nodes in these layers are very much alike (see Table 2 for their 90th to 100th percentile ranking). Possibly, the dynamics of the network within these temporal windows are indistinguishable. On the other hand, the ordinal relationship between the vulnerability ranking of nodes in some of the layers are very distinct. Extremely low correlation was exhibited between layers 2 and 20, layers 14 and 21, layers 8 and 15, etc. Majority of the entries in Table 1 are less than 0.50, this indicates that the criticality ranking of nodes in most of these layers are different. Collectively, we have demonstrated how the vulnerability indexes of various components of WDNs under extended period simulation vary in time (different temporal windows) using multilayer networks. It is impossible to capture these variabilities using steady state simulation and static networks.

4.2. Reduced multilayer vulnerability assessment

The hierarchical clustering algorithm briefly described in Section 2.2 seeks to maximize the relative entropy of the reduced multilayer network. Based on the distinguishability bar plot (relative entropy) amongst aggregated networks (Fig. 6), the original 24-layer network is best reduced into an 11 distinct layer network using the concept of structural reducibility of multilayers networks . A lot of reduced multilayer representations are possible, but none preserves the information contained in the original 24-layer network as compared to using this 11-layer network .

The optimally reduced multilayer network consist of layers aggregated from the original 24-layer network as follows; RdLayer 0 ←[layers 1, 2, 3 and 4], RdLayer 1 ← [layers 8 and 9], RdLayer 2 ← [layers 5, 6, 7, 10, 11, 12, 13, 14 and 15], RdLayer 3 ← [layers 0, 23] and rest 7 RdLayers are the same as layers 16, 17, 18, 19, 20, 21, and 22 of the original 24-layer network. This is due to the fact that these layers are distinct from one another. Since each original layer is represented as a directed graph which accounts for pipe flow and operational status of various assets in the WDN, the reduced multilayer network represents the aggregation of similar/identical temporal periods into a single layer. The dynamics of the WDN during the aggregated temporal periods are largely the same with little to no variation. This is particularly evident in RdLayer 0 ← [layers 1, 2, 3 and 4], RdLayer 1 ← [layers 8 and 9], and RdLayer 3 ← [layers 0, 23] implying that there is little to no variation in general dynamics of the WDN during the periods 1:00am – 4:00am, 8:00am – 9:00am and 11:00pm – 00:00midnight.

Fig. 7 presents the most important layers of the reduced multilayer network. In RdLayer 0, which is an aggregation of layers 1,2,3 and 4, Nodes 92 and 93 with their associated pumps are operational in the temporal window, 1:00am to 3:00am. During this period, Node 92 is highly vulnerable since it supplies more volume of water. Node 92 has the core mandate for filling the tanks in the network within this temporal window. The successors of Node 92 in the connectivity structure of the network are also deemed highly vulnerable. Failure of any of these nodes will have catastrophic consequences within this temporal window. Node 93 is the most vulnerable node in RdLayer 1 since Node 92 is using the bypass to supply water an indication that the tanks might be full. The temporal window of RdLayer 1, 8:00am to 9:00am, corresponds to early peak hours for demand as people get ready to start their daily activities. Structural reducibility is able to capture these interesting dynamics in the network.

In RdLayer 2, several layers (5,6,7,10,11,12,13,14 and 15) of the original multilayer network are aggregated. This implies that the dynamics of the network within the temporal windows specified by these layers are similar. The closed loop exhibited in RdLayer 2 is an indication that some of the layers aggregated have different directional flow between two successive nodes. RdLayer 2 is an aggregation of 9 layers so this is expected. This phenomenon does not in any way mean that dissimilar layers are aggregated. In the temporal window 11:00pm to 00:00 midnight, Node 93 and its associated pump are not operational as such they are isolated in Rdlayer 3. Failure of Node 93 will have no impact on the network within this temporal window. Node 92 is left with the ultimate responsibility of supplying the entire network and therefore ranked the most vulnerable node in RdLayer 3.

Table 3 presents the correlation between the layers present in the

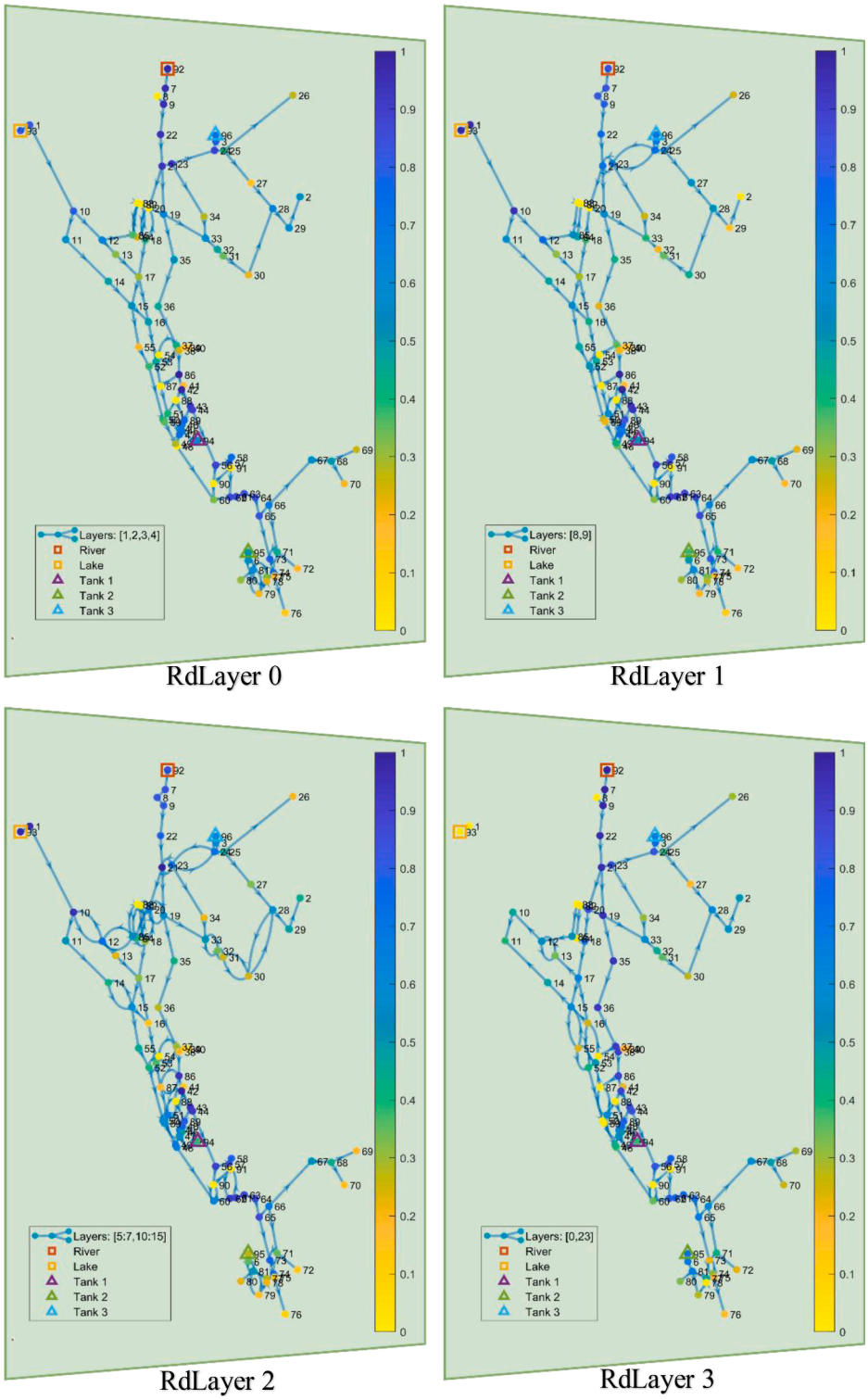

Fig. 7. Reduced layers 0, 1, 2 and 3 of Net 3.

reduced multilayer representation. A very high correlation is evident between RdLayers 4 and 5. This is not an indication of information redundancy in the reduced multilayer representation but rather due to the presence of many alternate paths for water to traverse in RdLayers 4 and 5. Two layers can have distinguishable flow directions but due to the looped nature of the network, failure of a particular node could result in identical connectivity loss and demand deficit created in these two layers of the network. Majority of the entries in Table 3 are less than 0.50, an indication that the criticality ranking of nodes in most of the reduced layer representation are different. The 90th to 100th percentile vulnerability ranking presented in Table 4 seem to vary form one reduced layer to another. However, the criticality ranking of some of the nodes persisted across all reduced layers. This is expected as the source (s) will always be highly vulnerable in each layer, irrespective of structural reducibility. This partially contributed to the fairly high correlation coefficient between some of the layers. Largely, the dynamics of the network can be summarised into these eleven distinct reduced multilayer representation.

Table 3
Kendall's rank correlation coefficient of reduced layers 0 to 10 of Net 3.

	RdL_0	RdL_1	RdL_2	RdL_3	RdL_4	RdL_5	RdL_6	RdL_7	RdL_8	RdL_9	RdL_{10}
RdL_0	1	0.705	0.721	0.585	0.295	0.296	0.307	0.306	0.282	0.274	0.388
RdL_1		1	0.845	0.425	0.399	0.399	0.402	0.389	0.319	0.305	0.324
RdL_2			1	0.480	0.422	0.422	0.421	0.411	0.338	0.311	0.370
RdL_3				1	0.373	0.374	0.381	0.435	0.534	0.571	0.717
RdL_4					1	0.989	0.981	0.931	0.781	0.727	0.340
RdL_5						1	0.982	0.933	0.781	0.728	0.342
RdL_6							1	0.921	0.789	0.735	0.349
RdL_7								1	0.841	0.791	0.408
RdL_8									1	0.938	0.524
RdL_9										1	0.578
RdL_{10}											1

Table 4
90th to 100th percentile vulnerability ranking of nodes in each reduced layer of Net3.

Rank	RdL_0	RdL_1	RdL_2	RdL_3	RdL_4	RdL_5	RdL_6	RdL_7	RdL_8	RdL_9	RdL_{10}
1	Node 86	Node 93	Node 93	Node 92	Node 49	Node 49	Node 50	Node 49	Node 20	Node 19	Node 21
2	Node 42	Node 42	Node 1	Node 7	Node 20	Node 20	Node 59	Node 20	Node 92	Node 35	Node 19
3	Node 92	Node 1	Node 42	Node 9	Node 48	Node 48	Node 49	Node 48	Node 57	Node 36	Node 35
4	Node 7	Node 10	Node 10	Node 22	Node 60	Node 60	Node 48	Node 60	Node 7	Node 37	Node 36
5	Node 9	Node 86	Node 43	Node 21	Node 50	Node 50	Node 20	Node 50	Node 50	Node 38	Node 37
6	Node 22	Node 43	Node 44	Node 19	Node 59	Node 59	Node 60	Node 92	Node 59	Node 86	Node 38
7	Node 21	Node 44	Node 86	Node 35	Node 62	Node 62	Node 92	Node 57	Node 49	Node 20	Node 86
8	Node 43	Node 56	Node 62	Node 36	Node 92	Node 92	Node 62	Node 59	Node 19	Node 92	Node 42
9	Node 23	Node 62	Node 56	Node 37	Node 57	Node 57	Node 57	Node 62	Node 8	Node 57	Node 92
10	Node 44	Node 61	Node 61	Node 38	Node 61	Node 61	Node 61	Node 7	Node 48	Node 50	Node 57

Table 5
Kendall's rank correlation coefficient between static and dynamic aggregate of Net 3.

	Static	Dynamic
Static	1	0.535
Dynamic		1

Table 6
90th to 100th percentile ranking of nodes in static and dynamic aggregate representation of Net 3.

Rank	Static	Dynamic
1	Node 92	Node 92
2	Node 7	Node 42
3	Node 9	Node 7
4	Node 22	Node 86
5	Node 21	Node 93
6	Node 19	Node 1
7	Node 35	Node 10
8	Node 36	Node 62
9	Node 37	Node 9
10	Node 38	Node 43

It is interesting to note that structural reducibility has aggregated similar layers based on the directional flow in the pipes and the operational status of the sources and their associated pumps. This is an interesting revelation and further lends credence to the fact that demand variations and the operational status of these components determine the dynamics of the network. Structural reducibility is known to reveal correlations, patterns and hidden dynamics in multilayer networks [45].

4.3. Static vs dynamic vulnerability assessment

To further highlight the merits of characterizing WDNs as multilayer networks and considering the dynamic aspect of the network in vulnerability assessment, we compared the proposed framework with a steady state static network vulnerability analysis of Net 3. Table 5 presents the ordinal relationship between the vulnerability ranking of nodes in the static representation and that of the proposed framework (dynamic aggregate). A correlation coefficient of 0.535 indicates the presence of significant difference in the vulnerability ranking of nodes when these two methods are compared. This is evident in Table 6, as only 3 of the nodes present in the 90th to 100th percentile vulnerability ranking of the dynamic approach are present in the static representation. The criticality ranking of the nodes was not accurately captured by the static network approach.

The vulnerabilities of Nodes 93 and 1 were not captured when the network is represented by a static network as depicted in Fig. 8. This is not an inherent flaw of DAVM but rather from a functional point of view, Nodes 93 and 1 do not contribute to the supply of water under a steady state simulation. Representation of WDNs as static networks and the consideration of steady state vulnerability analysis is actually just one of the numerous layers in the proposed multilayer framework which also makes use of extended period simulation. In the multilayer aggregate, the vulnerability of all components of the WDN were considered no matter how minuscule their operational time. The vulnerability of the Node 8 (bypass), Nodes 93 and 1 (the second source and its associated pump) and Nodes 94, 95 and 96 (Tanks 1, 2 and 3) were captured by the multilayer analysis. Clearly considering demand variations (extended period simulations) and the operational status of various components is a step in the right direction and an attempt to mimic the practical aspects of WDNs in vulnerability assessment.

The following practical implications can be drawn from this study. The proposed framework could be utilised as a tool by stakeholders of WDNs to assess the impact of various failure scenarios and prioritize maintenance routines. Specifically, the failure impact of each node can now be evaluated considering different temporal windows. Scheduled maintenance could be carried out in temporal windows where the vulnerability of the nodes/components are at their barest minimum. The framework could also help in the evaluation and diagnosis of system

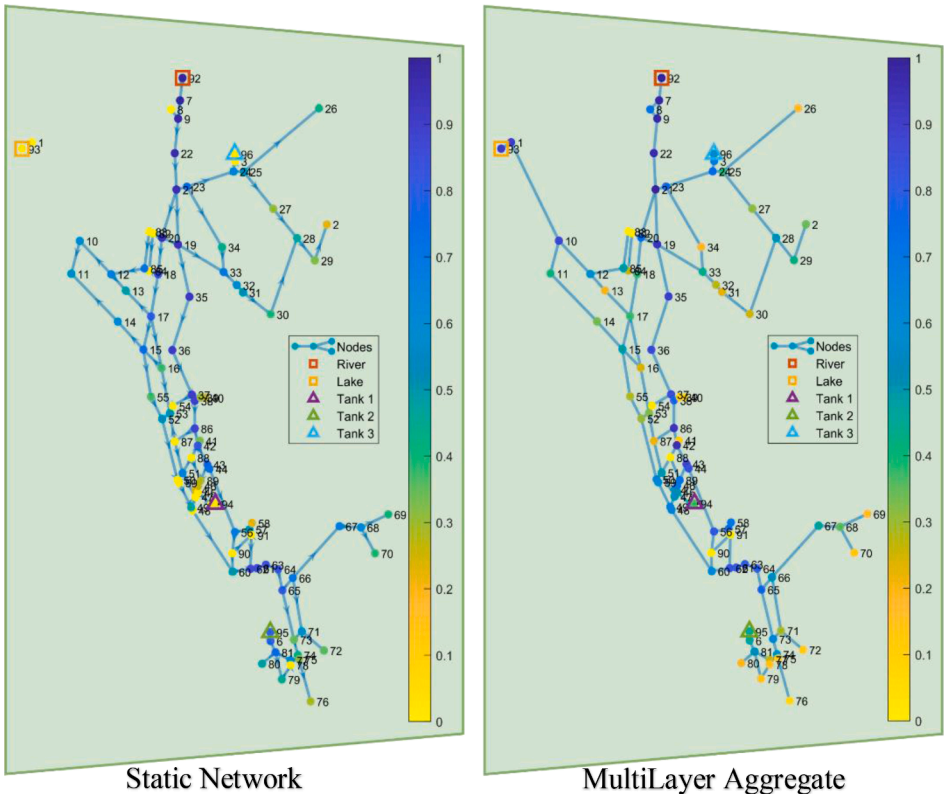

Fig. 8. Comparison Plot of Static and Multilayer dynamic aggregate vulnerability indexes.

reliability, prediction of system performance losses in relation to potential hazard scenarios, and the design of failure impact mitigation strategies. Cost effective monitoring strategies could also be implemented to monitor nodes with high failure impact in the WDNs using the proposed framework as a tool for node criticality assessment.

5. Conclusion

A systematic framework for dynamic nodal vulnerability assessment of WDNs based on multilayer networks and DAVM have been proposed and validated in this study. Utilising Net 3 as a case study, the following conclusions are made:

- The characterisation of each layer as a directed graph through the utilisation of flows in the pipes implies all hydraulic parameters are implicitly considered in the framework. This also helps ascertain the operational status of sources, pumps, valves etc. in the WDN.
- The importance of time, thus demand variations and the operational status of the various components of WDNs have been accounted for in the proposed vulnerability assessment framework via multilayer network representation.
- The vulnerability of each component of the WDN is captured in any given temporal window. This ensures that the criticality of components of the WDN that are not operational 24/7 are accurately captured.
- Structural reducibility of multilayer networks has demonstrated its ability to unearth hidden similarities, correlations and heterogeneity between different layers and reduce the computational burden of analysing many layers. Structural reducibility also buttresses the fact that the general dynamics of the WDN is influenced by demand variations and the operational status of sources, pumps, and valves.
- The two sources of Net 3, Nodes 92 and 93 and their associated pumps manifested in the 90th to 100th percentile vulnerability ranking of the proposed framework signifying how critical these components are to the WDN.

CRediT authorship contribution statement

Hoese Michel Tornyeviadzi: Conceptualization, Methodology, Software, Writing – review & editing. **Emmanuel Owusu-Ansah:** Methodology, Writing – review & editing. **Hadi Mohammed:** Conceptualization, Writing – review & editing. **Razak Seidu:** Supervision, Conceptualization, Methodology, Resources, Writing – review & editing.

Declaration of Competing Interest

The authors declare that they have no known competing financial interests or personal relationships that could have appeared to influence the work reported in this paper.

Acknowledgments

The findings of this study are practically reasonable and consistent with expectations in vulnerability assessment of WDNs. However, the study is not lacking limitations. Failure effects are confined to each temporal period. Future studies could look at the evolution of failure effects if not addressed in a timely fashion in the vulnerability assessment of WDNs.

This work was supported by the Smart Water Project (Project No: 90392200) funded by NTNU Smart Water Lab and Ålesund Municipality.

Supplementary materials

Supplementary material associated with this article can be found, in the online version, at doi:10.1016/j.ress.2021.108217.

References

[1] Faramondi L, Oliva G, Setola R. Multi-criteria node criticality assessment framework for critical infrastructure networks. Int J Crit Infrastruct Prot 2020;28:100338.
[2] Wang F, et al. Systemic vulnerability assessment of urban water distribution networks considering failure scenario uncertainty. Int J Crit Infrastruct Prot 2019;26:100299.
[3] Shuang Q, Zhang M, Yuan Y. Node vulnerability of water distribution networks under cascading failures. Reliab Eng Syst Saf 2014;124:132–41.
[4] Yazdani A, Jeffrey P. Water distribution system vulnerability analysis using weighted and directed network models. Water Resour Res 2012;48:6.
[5] Shirzad A, Tabesh M, Atayikia B. Multiobjective optimization of pressure dependent dynamic design for water distribution networks. Water Resour Manag 2017;31(9):2561–78.
[6] Giustolisi O, Ridolfi L, Simone A. Tailoring centrality metrics for water distribution networks. Water Resour Res 2019;55(3):2348–69.
[7] Wéber R, Huzsvár T, Hős C. Vulnerability analysis of water distribution networks to accidental pipe burst. Water Res 2020;184:116178.
[8] Meng F, et al. Topological attributes of network resilience: a study in water distribution systems. Water Res 2018;143:376–86.
[9] Yazdani A, Jeffrey P. Robustness and vulnerability analysis of water distribution networks using graph theoretic and complex network principles. In: Proceedings of the 12th annual conference on water distribution systems analysis; 2010. p. 933–45. 2010.
[10] Zarghami SA, Gunawan I, Schultmann F. Integrating entropy theory and cospanning tree technique for redundancy analysis of water distribution networks. Reliab Eng Syst Saf 2018;176:102–12.
[11] Agathokleous A, Christodoulou C, Christodoulou SE. Topological robustness and vulnerability assessment of water distribution networks. Water Resour Manag 2017;31(12):4007–21.
[12] Simone A, et al. Centrality metrics for water distribution networks. EPiC Ser Eng 2018;3:1979–88.
[13] Agathokleous A, Christodoulou C, Christodoulou S. Robustness and vulnerability assessment of water networks by use of centrality metrics. Eur Water Resour Assoc 2017;58:489–95.
[14] Balekelayi N, Tesfamariam S. Graph-theoretic surrogate measure to analyze reliability of water distribution system using bayesian belief network–based data fusion technique. J Water Resour Plan Manag 2019;145(8):04019028.
[15] Zarghami SA, Gunawan I, Schultmann F. Entropy of centrality values for topological vulnerability analysis of water distribution networks. Built Environ Proj Asset Manag 2019;9(3):412–25. https://doi.org/10.1108/BEPAM-02-2019-0014.
[16] Fei L, Deng Y. A new method to identify influential nodes based on relative entropy. Chaos Solitons Fractals 2017;104:257–67.
[17] Giudicianni C, et al. Topological placement of quality sensors in water-distribution networks without the recourse to hydraulic modeling. J Water Resour Plan Manag 2020;146(6):04020030.
[18] Nazempour R, Monfared MAS, Zio E. A complex network theory approach for optimizing contamination warning sensor location in water distribution networks. Int J Disaster Risk Reduct 2018;30:225–34.
[19] Zhou X, et al. Cycle based network centrality. Sci Rep 2018;8(1):1–11.
[20] Wang F, et al. Emergency repair scope partition of city water distribution network: a novel approach considering the node importance. Water Resour Manag 2017;31(12):3779–94.
[21] Wright R, et al. Hydraulic resilience index for the critical link analysis of multi-feed water distribution networks. Procedia Eng 2015;119:1249–58.
[22] Todini E. Looped water distribution networks design using a resilience index based heuristic approach. Urban Water 2000;2(2):115–22.
[23] Prasad TD, Park NS. Multiobjective genetic algorithms for design of water distribution networks. J Water Resour Plan Manag 2004;130(1):73–82.
[24] Di Nardo A, et al. Redundancy features of water distribution systems. Procedia Eng 2017;186:412–9.
[25] Tanyimboh TT, et al. Comparison of surrogate measures for the reliability and redundancy of water distribution systems. Water Resour Manag 2016;30(10):3535–52.
[26] Gunawan I, Schultmann F, Zarghami SA. The four Rs performance indicators of water distribution networks. Int J Qual Reliab Manag 2017;34(5):720–32. https://doi.org/10.1108/IJQRM-11-2016-0203.
[27] Guidotti R, Gardoni P, Rosenheim N. Integration of physical infrastructure and social systems in communities' reliability and resilience analysis. Reliab Eng Syst Saf 2019;185:476–92.
[28] Zarghami SA, Gunawan I. A domain-specific measure of centrality for water distribution networks. Eng Constr Archit Manag 2019;27(2):341–55. https://doi.org/10.1108/ECAM-03-2019-0176.
[29] Wei Y, Liu X. A path-based entropic resilience assessment method for nodes in water supply networks. In: Proceedings of the IIE annual conference. Institute of Industrial and Systems Engineers (IISE); 2017.
[30] Maiolo M, et al. A new vulnerability measure for water distribution network. Water 2018;10(8):1005.
[31] Tabesh M, Tanyimboh TT, Burrows R. Extended period reliability analysis of water distribution systems based on head driven simulation method. In: Proceedings of the bridging the gap: meeting the world's water and environmental resources challenges; 2001.
[32] Kivelä M, et al. Multilayer networks. J Complex Netw 2014;2(3):203–71.
[33] Boccaletti S, et al. Complex networks: structure and dynamics. Phys Rep 2006;424(4–5):175–308.
[34] Dickison ME, Magnani M, Rossi L. Multilayer social networks. Cambridge University Press; 2016.
[35] Cardillo A, et al. Emergence of network features from multiplexity. Sci Rep 2013;3(1):1–6.
[36] De Domenico M, et al. Navigability of interconnected networks under random failures. Proc Nat Acad Sci 2014;111(23):8351–6.
[37] Huang Z, et al. Modeling cascading failures in smart power grid using interdependent complex networks and percolation theory. In: Proceedings of the IEEE 8th conference on industrial electronics and applications (ICIEA). IEEE; 2013.
[38] Cuadra L, et al. A critical review of robustness in power grids using complex networks concepts. Energies 2015;8(9):9211–65.
[39] de Arruda GF, et al. Disease localization in multilayer networks. Phys Rev X 2017;7(1):011014.
[40] Cozzo E, et al. Contact-based social contagion in multiplex networks. Phys Rev E 2013;88(5):050801.
[41] Bianconi G. Statistical mechanics of multiplex networks: entropy and overlap. Phys Rev E 2013;87(6):062806.
[42] De Domenico M, et al. Ranking in interconnected multilayer networks reveals versatile nodes. Nat Commun 2015;6(1):1–6.
[43] Estrada E, Gómez-Gardenes J. Communicability reveals a transition to coordinated behavior in multiplex networks. Phys Rev E 2014;89(4):042819.
[44] Granell C, Gómez S, Arenas A. Dynamical interplay between awareness and epidemic spreading in multiplex networks. Phys Rev Lett 2013;111(12):128701.
[45] Domenico MD, et al. Structural reducibility of multilayer networks. Nat Commun 2015;6(1):1–9.
[46] Sánchez-García RJ, Cozzo E, Moreno Y. Dimensionality reduction and spectral properties of multilayer networks. Phys Rev E 2014;89(5):052815.
[47] Battiston F, Nicosia V, Latora V. Structural measures for multiplex networks. Phys Rev E 2014;89(3):032804.
[48] Bianconi G. Multilayer networks: structure and function. Oxford university press; 2018.
[49] D'Agostino G, Scala A. Networks of networks: the last frontier of complexity, 340. Springer; 2014.
[50] Ward JH. Hierarchical grouping to optimize an objective function. J Am Stat Assoc 1963;58(301):236–44.
[51] Liu C, Wu J. Scalable routing in cyclic mobile networks. IEEE Trans Parallel Distrib Syst 2008;20(9):1325–38.
[52] Rossman, L. A. (1994). EPANET users manual.
[53] WDS- Research Database. Water Distribution System Research Database. 2020; Available from: http://www.uky.edu/WDST/database.html.
[54] Eliades DG, et al. EPANET-MATLAB toolkit: an open-source software for interfacing EPANET with MATLAB. In: Proceedings of the 14th international conference on computing and control for the water industry, CCWI; 2016.